• SUPPLEMENTARY INFORMATION

Unraveling the Time Course of Interaction between DNA Nanopores and Lipid Bilayers using QCM-D: Role of Cholesterol Anchors and Bilayer Supporting Substrates

Zugui Peng [a*], Glenn Villena Latag [b], Hiroyuki Tahara [b], Tohru Yagi [a*], and Tomohiro Hayashi [b*]

[a] *Department of Mechanical Engineering, School of Engineering, Institute of Science Tokyo, 403, Ishikawadai Bldg. 3, 2-12-1 Ookayama, Meguro-ku, Tokyo 152-8550, Japan*

[b] *Department of Materials Science and Engineering, School of Materials and Chemical Technology, Institute of Science Tokyo, 4259 Nagatsuta-Cho Midori-Ku, Yokohama, Kanagawa 226-8502, Japan*

Table S1. Water contact angles of modified QCM-D sensor and coverslip (n = 3). Water contact angle measurements showed an increase in surface hydrophobicity after the treatment with PEG and palmitic acid, which confirmed successful surface modification[1]. The water contact angle of the coverslip was found to be lower compared with the SiO_2, which might be due to the lower purity of the coverslips.

Compound	QCM-D sensor	Coverslip
PEG	28.3 ± 0.1°	21.7 ± 0.01°
Palmitic acid	51.5 ± 0.03°	43.2 ± 0.4°

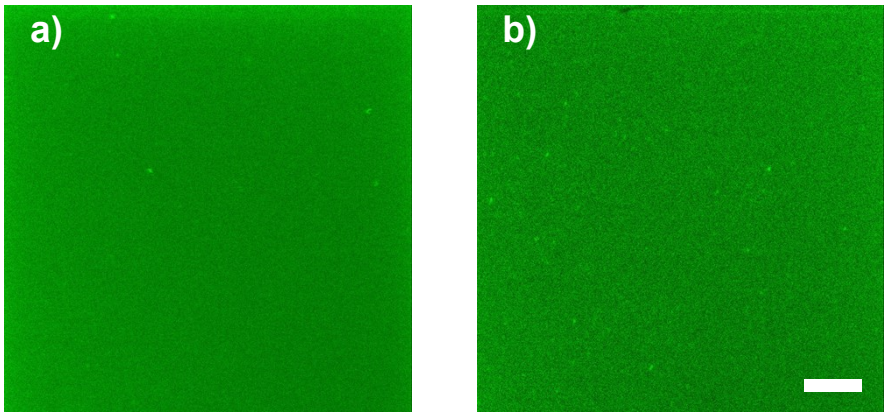

Figure S1. Representative fluorescence images of SLBs formed on (a) SiO_2 and (b) PEG. The areas with high fluorescence intensity are membrane protrusions. The diffusion coefficients *D* are shown below the images (n = 5). The scale bar represents 5 μm. Compared with the bilayer formed on SiO_2, more protrusions with high fluorescence intensity were observed on SLBs formed on PEG, suggesting some unruptured SUVs stacked on the PEG surface. However, with the FRAP experiment, we found the diffusion coefficients of bare SiO_2 (1.7 ± 0.1 $\mu m^2/s$) and PEG-modified surface (1.8 ± 0.1 $\mu m^2/s$) are statistically insignificant ($p>0.05$). Hence, the membrane protrusions may only have a small impact on the membrane fluidity.

1. TABLES AND FIGURES

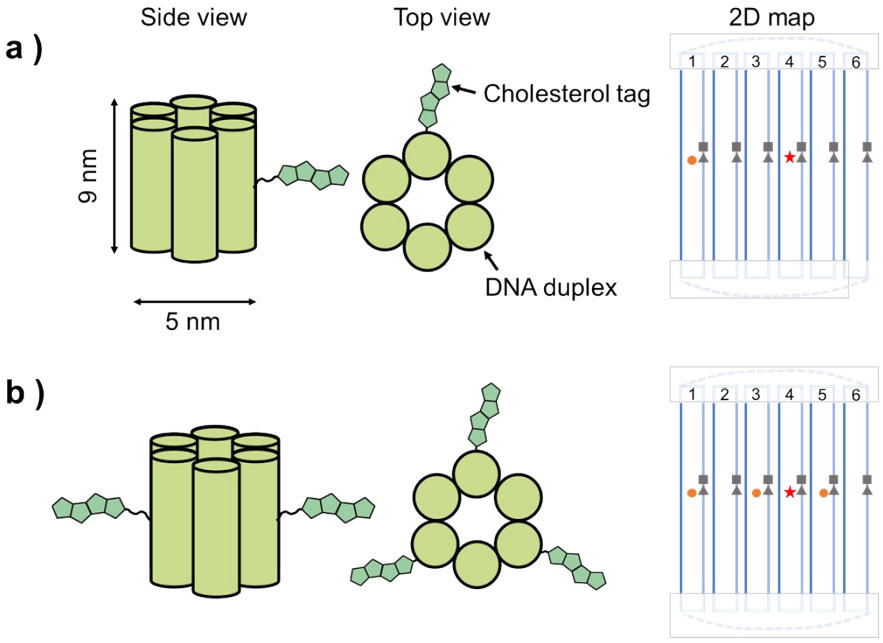

Figure S2. Side view, top view and 2D map of (a) DNP-1C and (b) DNP-3C. The nanopores are composed of six DNA duplexes and has a dimension of 9 nm in height and 5 nm in outer diameter. Orange circles in 2D map indicate cholesterol tags, the red stars show Cy3 fluorophore. Squares and triangles represent the 5' and 3' termini of the strands. The semi-transparent strands indicate the T_4 hair-pin loop.

Table S2. ID, sequences and chemical modification of the DNA strands used for DNA nanopores.

ID	Sequences (5' → 3')
1	AGCGAACGTGGAGTCCGACATCGGCAAGCTCCCTCGACTATT
2	CCGATGTCGGACACACGATCTTCGCCTGCTGGGGGGAGCTTG
3	CGAAGATCGTGTCCACAGTTGATTGCCCTTCACCCCAGCAGG
4	AATCAACTGTGGTCTCACTGGTGATTAGAATGCGTGAAGGGC-TEG Cy5
5	TCACCAGTGAGATGTCGTACCAGGTGCATGGATGCATTCTAA
6	CCTGGTACGACATCCACGTTCGCTAATAGTCGAATCCATGCA
1C	Sequence of 1 carrying a cholesterol via TEG linker at the 3' terminus
3C	Sequence of 3 carrying a cholesterol via TEG linker at the 3' terminus
5C	Sequence of 5 carrying a cholesterol via TEG linker at the 3' terminus

Table S3. Names and composition of DNA nanopores.

Nanopore	Oligonucleotides used
DNP-0C	1, 2, 3, 4, 5, 6
DNP-1C	1, 2, 3C, 4, 5, 6
DNP-3C	1C, 2, 3C, 4, 5C, 6

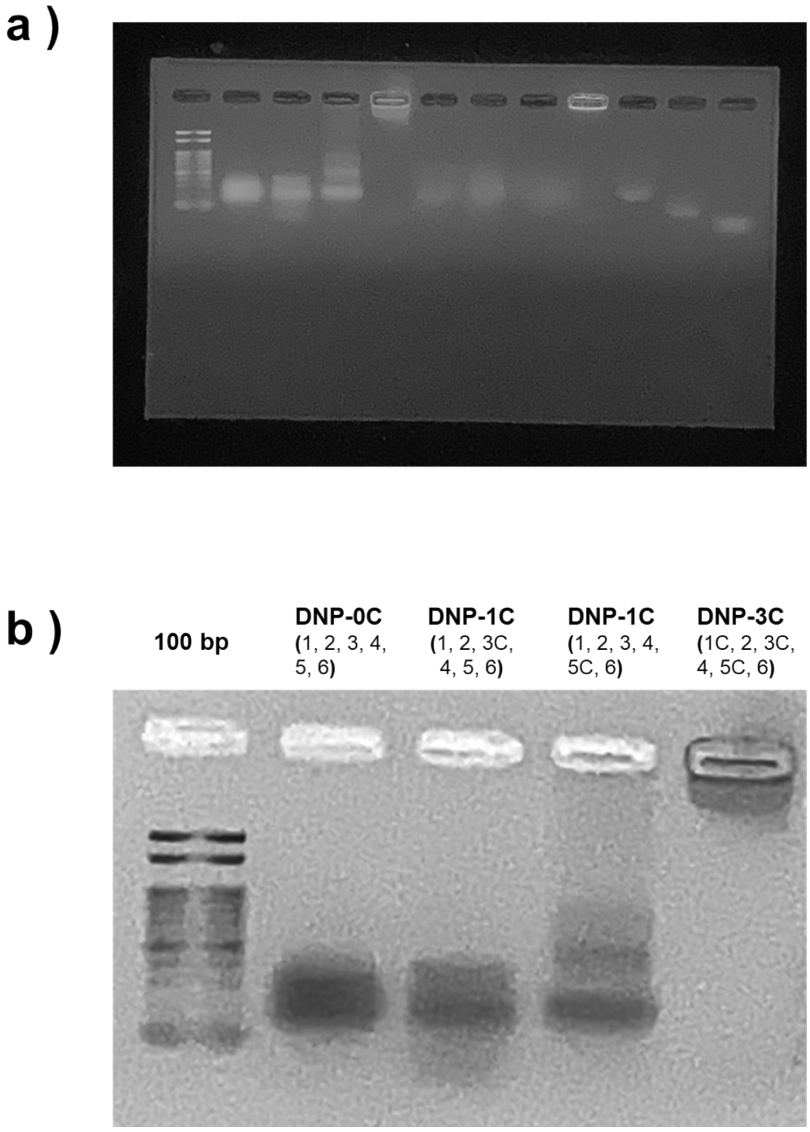

Figure S3. Original (a) and processed (b) images of 2% agarose gel electrophoresis of assembled DNA nanopores. 100 bp DNA ladder was used as a molecular weight marker and DNA nanopores without cholesterol tag modification (DNP–0C) were used as a control. The hydrophobic interaction between cholesterol tags results in the aggregation of DNPs. Hence, the small aggregation of DNP-1C led to band smearing, while the large aggregation of DNP-3C caused no migration. Only lanes 1–5 in (a) were processed and zoomed in (b), as lanes 6–12 contain samples from a different experiment. We tested two variants of DNP-1C, each composed of different cholesterol-modified oligonucleotides.

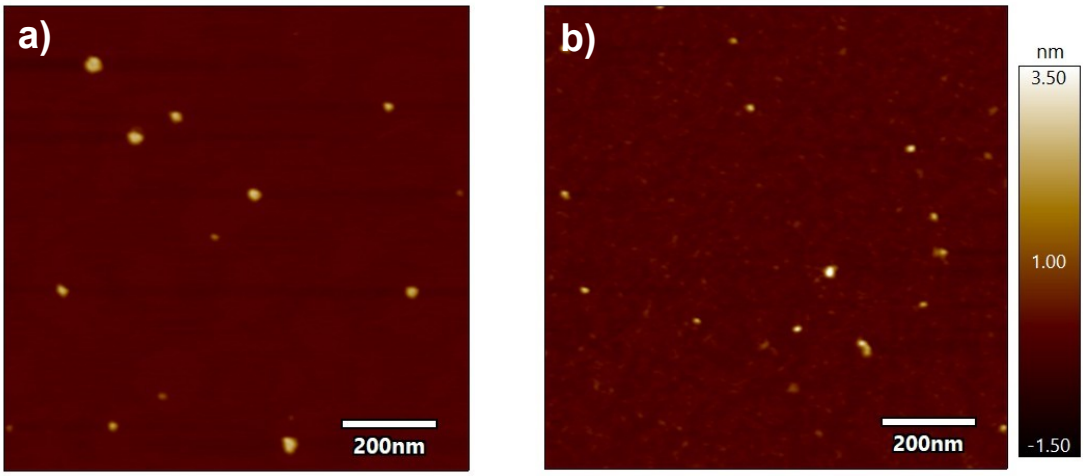

***l* = 9.4 ± 3.8 nm** ***l* = 8.3 ± 3.1 nm**

Figure S4. Representative AFM images of (a) DNP-1C and (b) DNP-3C. The lengths *l* of the NPs are shown below the images (n = 12). After correction of the tip convolution effect, the outer diameter (*l*) of DNP-1C and DNP-3C were found to be 9.4±3.8 nm and 8.3±3.1 nm (n = 12), respectively, and are in good agreement with the theoretical length.

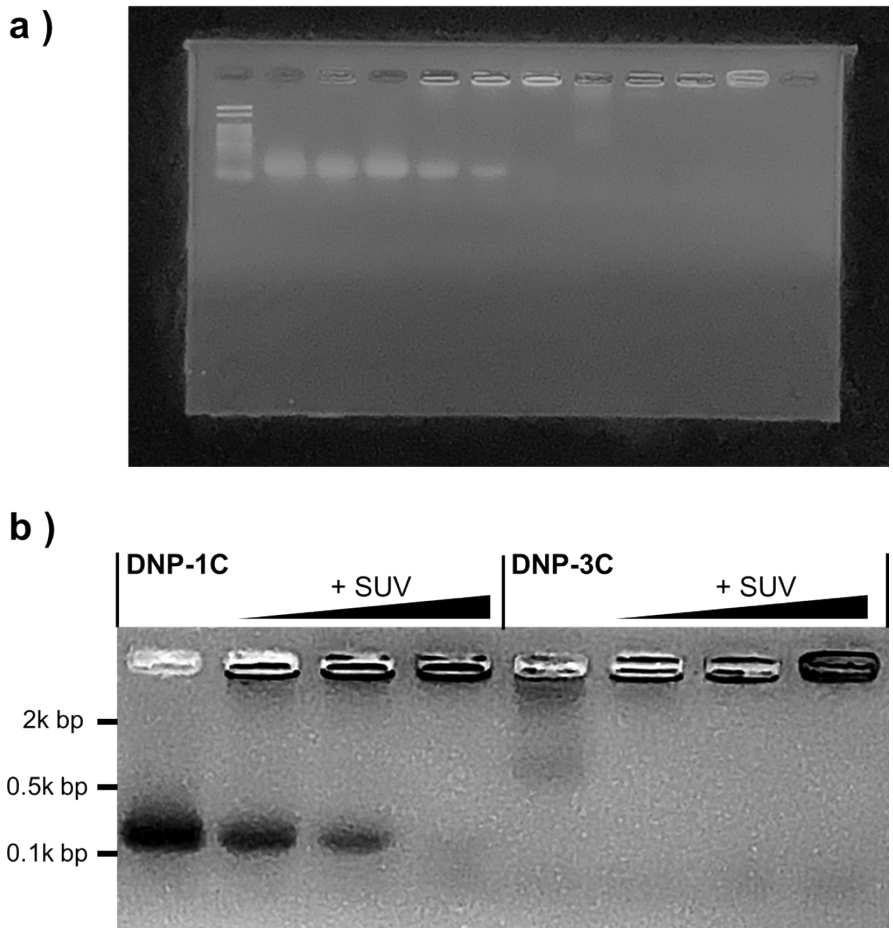

Figure S5. Original (a) and processed (b) images of SUV binding assay of DNP-1C and DNP-3C. Increasing the concentration of SUV leads to more DNA nanopores binding to the SUV. The position and bp length of the DNA ladders are shown at the left of the gels. The SUV-bound DNPs are not able to migrate into the gel, hence a higher concentration of SUV-bound DNPs leads to a clearer band at the top of the gel. As a result, a band of DNP-1C shifted up only at a high SUV concentration, while DNP-3C bonded to the SUV even at a low SUV concentration. This result follows that DNP-1C has a weaker interaction with the SLBs than DNP-3C as discussed above.

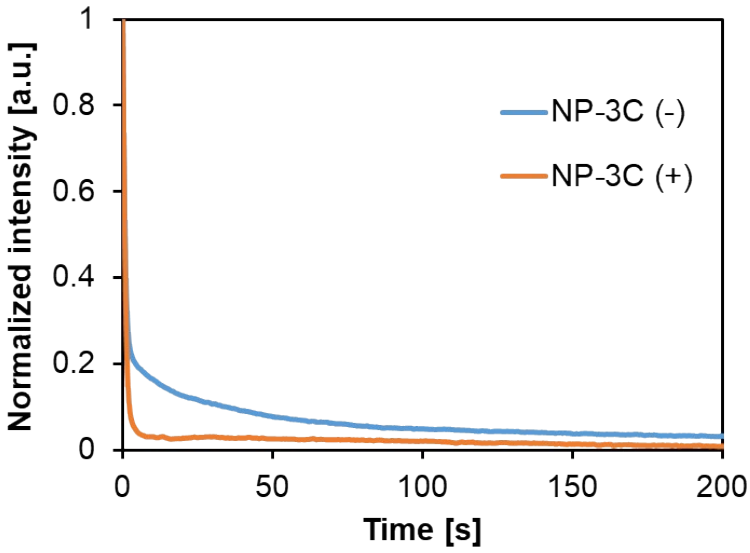

Figure S6. Time traces of normalized HPTS fluorescence intensity after exposing the SUV to the external buffer. DNP-3C (+) and DNP-3C (-) represent SUV incubated with and without DNP-3C, respectively. The faster HPTS fluorescence decay in SUVs incubated with DNP-3C suggested proton transport across the pore.

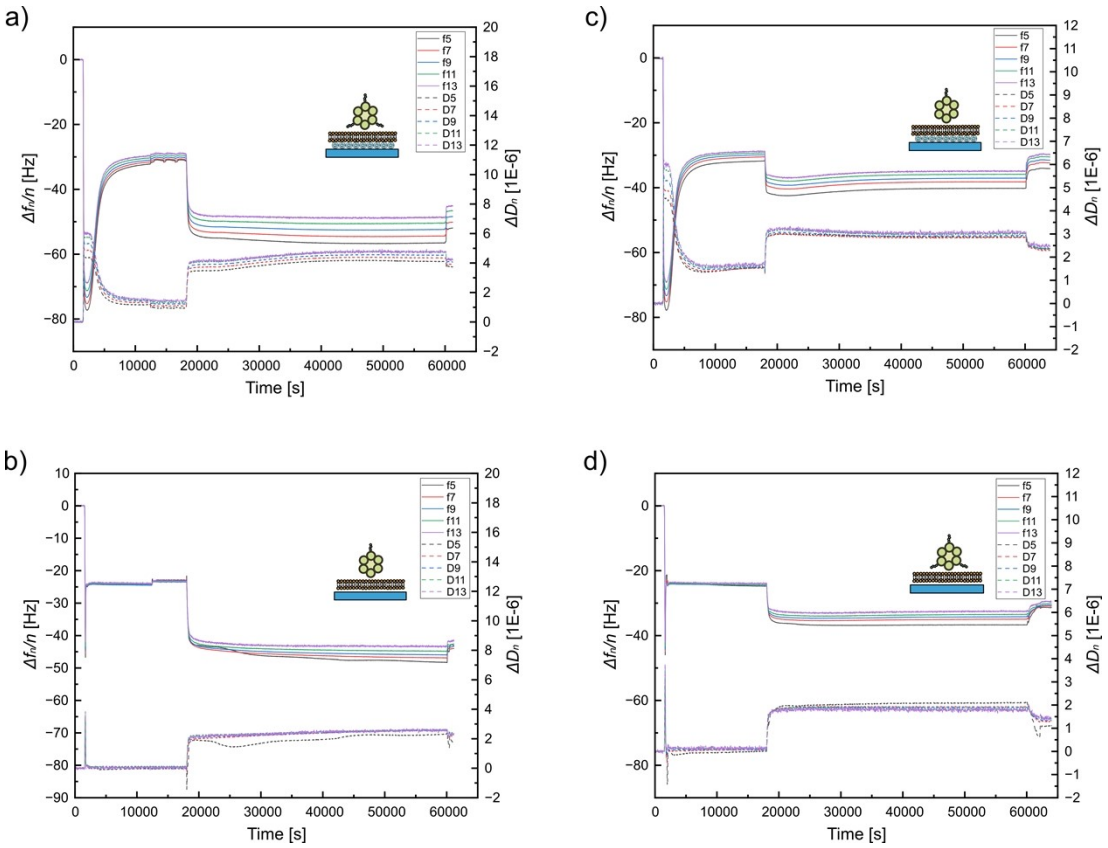

Figure S7. Shifts in energy dissipation (dashed line) and normalized frequency (solid line) for DNP-3C and DNP-1C interacting with SLBs supported by PEG (a) (b), and for SLBs supported by SiO_2 (c) (d) from 5^{th} to 13^{th} overtone.

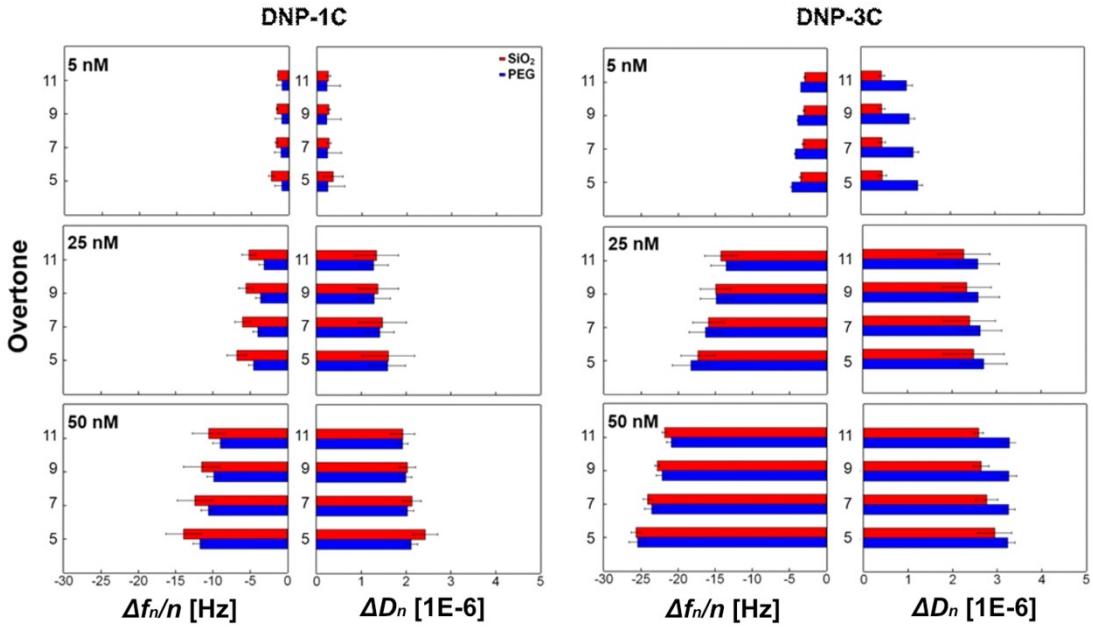

Figure S8. Changes in $\Delta f_n/n$ and ΔD_n at various concentrations of DNP-1C (left) and DNP-3C (right) interacting with SLBs supported by SiO_2 (red) and PEG (blue). Initial measurement was taken from DNA nanopores injection and final measurement was taken after DNP injection. Data were collected from 5th through 11th overtone. Error bars represent the standard deviation (n = 3).

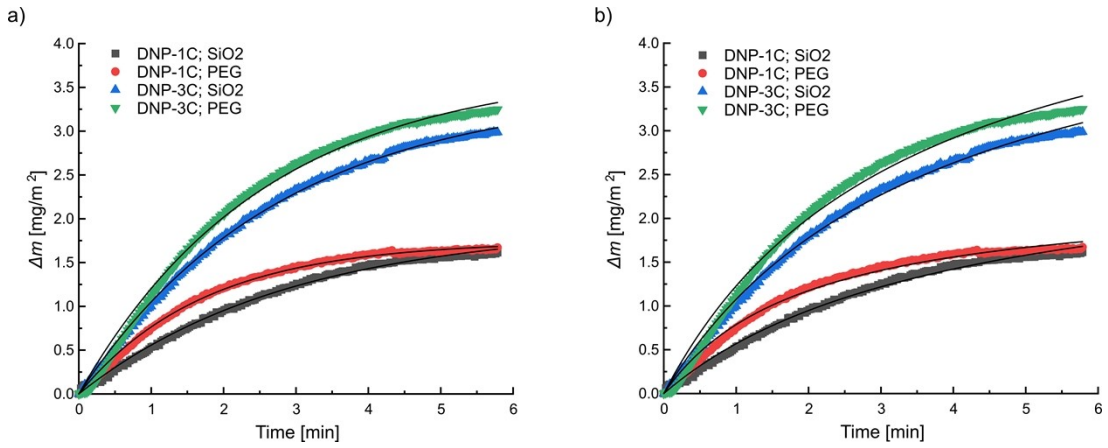

Figure S9. Pseudo-first-order (a) and pseudo-second-order (b) plots for DNP-1C and DNP-3C adsorption on SLBs supported by SiO_2 and PEG substrate. The points were the experimental data, and the solid lines were the fitting results.

Table. S4 Fitting parameters for DNP-3C and DNP-1C adsorption on SiO_2 and PEG-supported SLBs at 50 nM using pseudo-second-order-model.

	q_s (mg/m^2)	q_e (mg/m^2)	k (1/min)	R^2
DNP-1C; SiO2	1.61	2.85	0.09	0.994
DNP-3C; SiO2	2.98	5.08	0.05	0.997
DNP-1C; PEG	1.67	2.36	0.22	0.991
DNP-3C; PEG	3.24	5.38	0.05	0.989

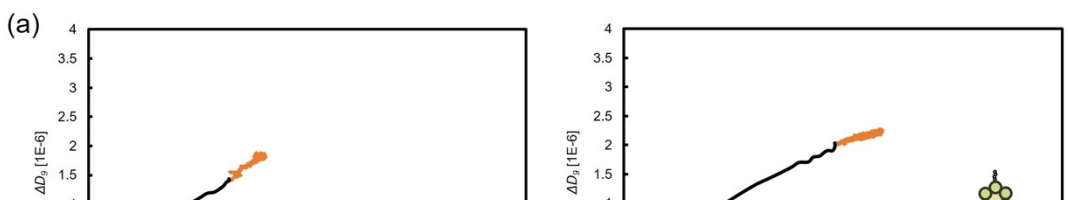

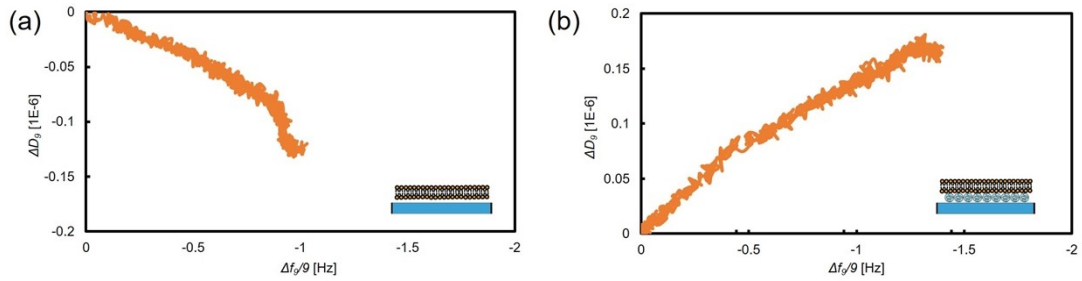

Figure S11. Other results of ΔD_9 versus $\Delta f_9/9$ plot showing shifts in ΔD_n and $\Delta f_n/n$ for SLBs supported by SiO_2 (a) and PEG (b) for 10 h.